Research Article

IJCRCPS

Growth, XRD, spectral and thermal studies on diethylammonium pentachlorostrontium(II) crystal

K.Kanagavalli[1], D.M.Muniraj[2], T.Dhanabal[3]

[1]Department of Chemistry, Info Institute of Technology, Kovilpalayam, Coimbatore-641 107, Tamil Nadu, India.
[2]Department of Chemistry, Government Arts and Science College, Pappireddipatti, Dharmapuri-636905, Tamil Nadu, India.
[3]Department of Chemistry, Muthayammal College of Engineering, Rasipuram, Namakkal-637408, Tamil Nadu, India
*Corresponding author: E-mail: dhanabal27@gmail.com;
Fax: +91 4287 226537; Tel: +91 6381225337.

Abstract

The title crystal has been successfully prepared and single crystals were obtained from saturated aqueous solution by slow evaporation method at room temperature. The results of the elemental analysis of the crystal agree with the stoichiometry ratio of the crystal. The sharp and well defined Bragg peaks observed in the powder X-ray diffraction pattern confirm its crystallinity. Thermal analyses (TG and DTA) were carried out to characterize the thermal behavior and stability of crystal. The results of differential thermal analysis (DTA) conform to the results of TGA. The weight losses observed were suitably explained based on the formulated decomposition pattern by using TG-DTA thermogram. The characteristic functional groups in the crystal were identified from Fourier transform infrared spectroscopy. The ^{1}H spectrum was recorded to establish the molecular structure of the title crystal. The powder SHG efficiency of the crystal was carried and found that the crystal possess SHG efficiency behavior. The DFT calculation study was studied to find out the HOMO-LUMO energy gap and intra-molecular charge transfer (ICT) interaction occurs within the molecule. Further investigations on the ferroelectric and dielectric behavior of the crystal at low temperatures are in progress.

1. Introduction

The importance of A_2BX_5 crystals (where A = univalent cation, NH_4^+ and its alkyl derivatives; B = divalent transition metal cation and X = halogen) has been realized in recent years owing to their interesting physical properties like ferroelectric, ferroelastic and commensurate-incommensurate phase transitions at low temperatures. Many compounds of this family represent the largest group of insulating crystals with structurally incommensurate phases [1, 2]. Many authors have reported successive phase transitions and ferroelectricity at low temperatures for copper compounds like $[N(CH_3)_4]_2CuCl_4$, $[N(CH_3)_4]_2CuBr_4$ and $[N(C_2H_5)_4]_2CuBr_4$ [3,4]. The dielectric measurements that the phase transitions in $[N(C_2H_5)_4]_2CuCl_4$ at 259K is of first order [5]. Another interesting subclass in this series is the dihydrated crystals. [6,7]. Hydrated crystals of the type $A_2BX_4.2H_2O$ and $A_3BX_5.2H_2O$ are also interesting class of compounds as they show a number of successive phase transitions at low temperatures. Raman scattering study on $[NH_4]_2CuCl_4.2H_2O$ crystals at low temperatures also studied. The phase transitions occurring in $(NH_4)_3BaCl_5.2H_2O$ is due to the stepwise dehydration of the two water molecules of crystallization [8]. The high pressure Brilliouin scattering and energy disperse X-ray diffraction study on the proto type compound, $[NH_4]_2ZnCl_4$ ranging from room temperature to 100°C. At ambient pressure three phase transitions occur in this temperature range in the compound [9].

Asurvey of literature reveals that for many of these crystals the thermal studies and spectral studies (DTA, FTIR and NMR) were not carried out. Many of these crystals not synthesized so far. In this paper, we report the synthesis and characterization of diethylammonium pentachlorostrontium(II) $[(C_2H_5)_2NH_2]_2SrCl_5,$ crystals (hereafter abbreviated as (DEAPC-Sr). The synthesized crystal characterized through CHNS, PXRD, Emission, TG, DTA, NMR, FTIR,

Polarized Raman, NLO and DFT studies. The ferroelectric and dielectric and single crystal X-ray structural analysis of the crystal are under progress.

2.2. Experimental methods

2.2.1 Growth of single crystal of DEAPC-Sr

The single crystals of diethylammonium pentachlorostrontium(II) (DEAPC-Sr) were grown by slow evaporation of the saturated aqueous solutions at room temperature. Three moles of diethylammoniumchloride and one mole of strontium (II) chloride hexahydrate react to form DEAPC-Sr crystals. Aqueous solutions containing analytical grades of diethylammoniumchloride and strontium (II) chloride hexahydrate in 3:1 molar ratio respectively were prepared separately by using triply distilled water. The two solutions were mixed together well and the resulting solution was filtered through a Whatman 42 filter paper into a clean dry beaker. The beaker was covered by an ordinary filter paper. Care was taken to minimize the temperature gradient and mechanical shock.

Three moles of diethylammoniumchloride and one mole of strontium (II) chloride hexahydrate react to form DEAPC-Sr crystals taking one mole of water from the aqueous solution according to the following equation.

$$2[(C_2H_5)_2NH_2]Cl \ + \ SrCl_2.6H_2O \longrightarrow [(C_2H_5)_2NH_2]_2SrCl_5$$
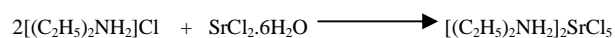
DEAPC-Sr

Bright, transparent, needle-shaped and colourless DEAPC-Sr crystals were obtained. Crystallization took place within 15 to 25 days under the experimental conditions. The grown crystals were collected from the mother liquid by using well cleaned forceps. The harvested crystals were recrystallized repeatedly to get crystals of good quality. The photograph of the grown crystals of DEAPC-Sr is shown in Figure 1.
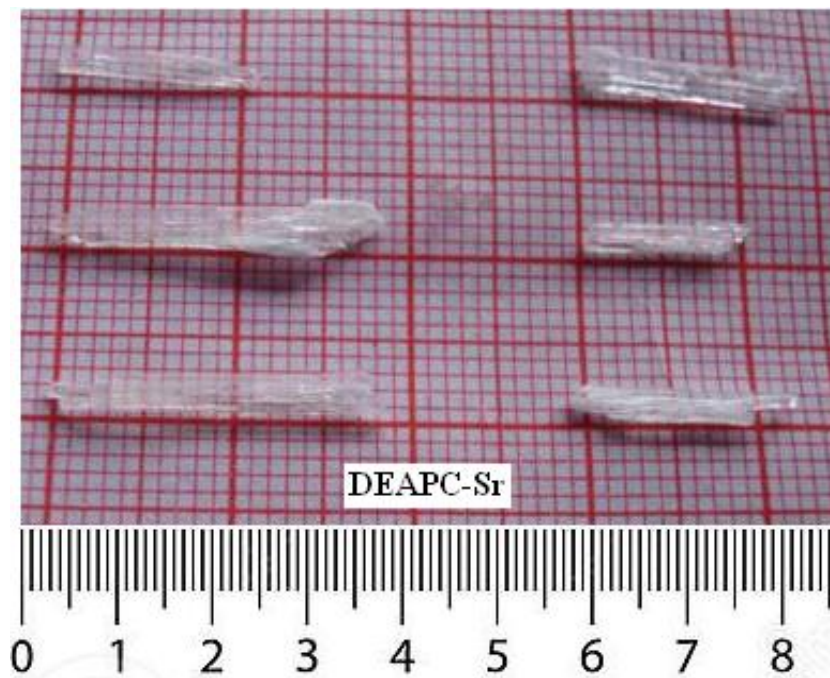
Figure 1. Photograph of DEAPC-Sr crystal.

2.1. Characterization techniques

The elemental analysis of the crystal is recorded at using Vario EL III CHNS instrument at Sophisticated Test and Instrumentation Centre, Cochin University of Science and Technology, Cochin. The powder XRD patterns of DEAPC-Sr crystal was obtained using BRUKER AXS D8 Advance X-ray diffractormeter model instrument with Cu K radiation (= 1.54060 Å) in room temperature at STIC (Sophisticated Test and Instrumentation Centre) Cochin. The thermal analyses (TG and DTA) were recorded at STIC, Cochin using a PERKIN ELMER DIAMOND thermal analyzer under nitrogen atmosphere. The sample was heated from room temperature to 1020ºC at a heating rate of 10ºC per minute. The FTIR spectra the crystal was recorded at SRMV College of Arts and Science, Coimbatore using a Perkin Elmer model RX1 instrument. The NMR spectrum of DEAPC-Sr crystal was carried out using Bruker AVIII 500 MHz NMR instrument model at IIT, Madras. The second harmonic generation efficiencies of the complexes were carried out by modified Kurtz-Perry powder technique using Nd:YAG laser, IISc, Bangaluru. The DFT study of the crystal was studied by quantum chemical descriptors.

3. Results and discussion

3.1. C H N S analysis

The elemental analysis data of the grown crystal is given in Table 1. Elemental analysis was recorded to determine the purity and compositions of the crystal. The experimental and calculated percentage of C H and N are very close to each other. The close agreement between the experimental and calculated values of C H and N confirms the formation of the crystal in the stoichiometric ratio.

24

Table 1. Elemental analysis data of DEAPC-Sr crystal.

Element	Carbon	Hydrogen	Nitrogen
Experimental	42.93	5.81	6.78
Calculated	42.87	5.78	6.69

3.2. Powder X-ray diffraction

The powder diffraction pattern of DEAPC-Sr is depicted in Figure 2. The experimental values of 2θ, d and I are given in Table 2. The sharp and well defined Bragg peaks at specific 2θ angles in the powder X-ray diffraction pattern confirm the crystalline nature of the crystal. The title is indexed using CRYSFIRE software. The crystal belongs to monoclinic system with cell parameters, a = 13.8570 Å, b = 12.2896 Å, c = 11.5790Å and ζ = = = 90 . The unit cell volume is 1971.91Å^3. The compound $SrCl_2.6H_2O$ is belongs to trigonal system. The crystal system of the synthesized crystal, DEAPC-Sr is entirely different from $SrCl_2.6H_2O$ crystal system that indicates the formation of DEAPC-Sr crystal.
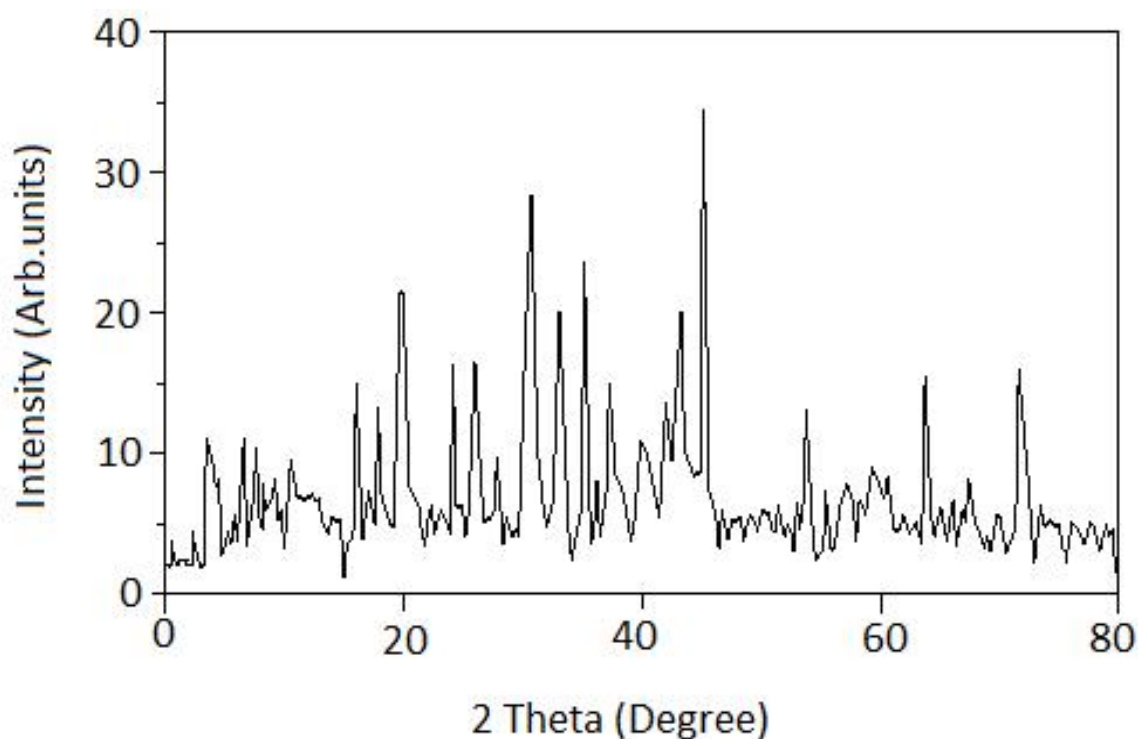

**Figure 2.** Powder X-ray diffraction pattern of DEAPC-Sr crystal.

25

Table 2. Powder X-ray diffraction pattern of DEAPC-Sr crystal.

Peak	2 (deg)	d (Å)	I Arb.units
1	16.53	13.51	11.2
2	16.10	5.49	14.9
3	19.64	4.51	21.3
4	24.21	3.67	16.1
5	26.03	3.41	16.4
6	30.65	2.86	28.3
7	32.95	2.71	20.1
8	35.17	2.54	23.5
9	37.23	2.41	14.8
10	43.27	2.08	20.1
11	45.21	2.00	34.3
12	53.85	1.70	12.9
13	63.81	1.44	15.4
14	71.68	1.31	16.1

3.3 Thermal studies

3.3.1 TG analysis

The TG thermogram of DEAPC-Sr crystal is shown in Figure 3. The crystal DEAPC-Sr decomposes in single stage when heated from room temperature to 1020°C at a heating rate of 10°C per minute at nitrogen atmosphere. Following decomposition pattern has been formulated to account for the weight loss observed.

$$[(C_2H_5)_2NH_2]_2SrCl_5 \xrightarrow{\text{90-190°C}} NH_2$$
$$_+Cl_2 + [(C_2H_5)_2]_2NH_2.SrCl_3$$
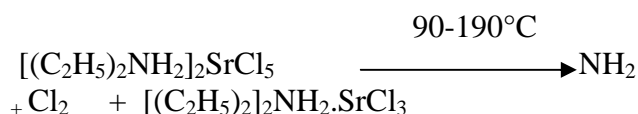
Molecular weight: 412.87

Experimental weight loss: 18%

Calculated weight loss: 20.87%

The TG thermogram shown in Figure 3 shows a single stage weight loss occurs between 90°C and 190°C. The crystal is stable upto at 90°C. Afterwards it decomposes slowly. The weight loss is due to loss of one molecule of NH_2 and one molecule of Cl_2 from a molecule of $[(C_2H_5)_2NH_2]_3SrCl_5$. The experimental weight loss for the step is 18%. The calculated weight loss for the step is 20.87%. The difference between the experimental and the formulated weight loss stage is small. The small difference in weight loss may due to the some adsorbed and occluded water molecules in the crystal. The crystal, $[(C_2H_5)_2]_2NH_2.SrCl_3$ as such after the temperature 190°C. Based this decomposition pattern of the this crystal, this synthesized crystal can be uded for optoelectronic application and also this crystal may has high mechanical stability.
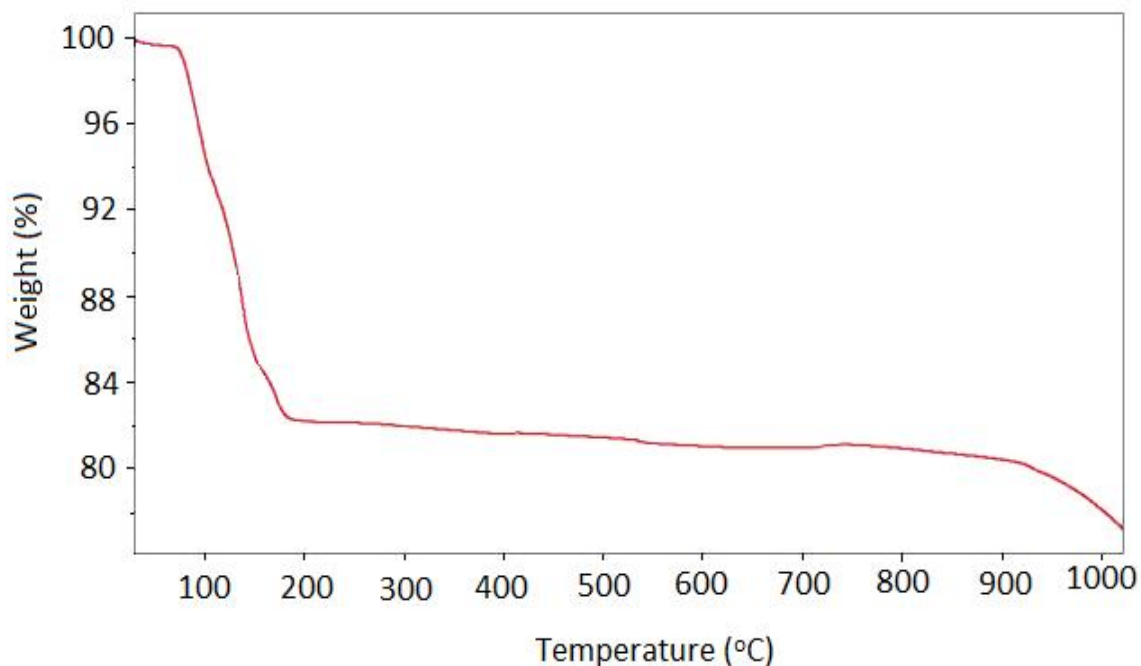
Figure 3. TG thermogram of DEAPC-Sr crystal.

3.3.2 DTA analysis

DTA curve of the crystal DEAPC-Sr is shown in Figure 4. On heating DEAPC-Sr crystal at rate of 10°C per minute three exothermic peaks appears between at 100°C and 140°C. The first exothermic peak at 100°C is due the elimination of the absorbed and occluded water molecules. The second exothermic peak at 155°C is due to the decomposition of the crystal. The third exothermic peak at 915°C may be due to the melting point of the $SrCl_2$. The DTA study thus conforms to the TG study. The TG and DTA studies confirm the formation of the compound in the stoichiometric ratio.
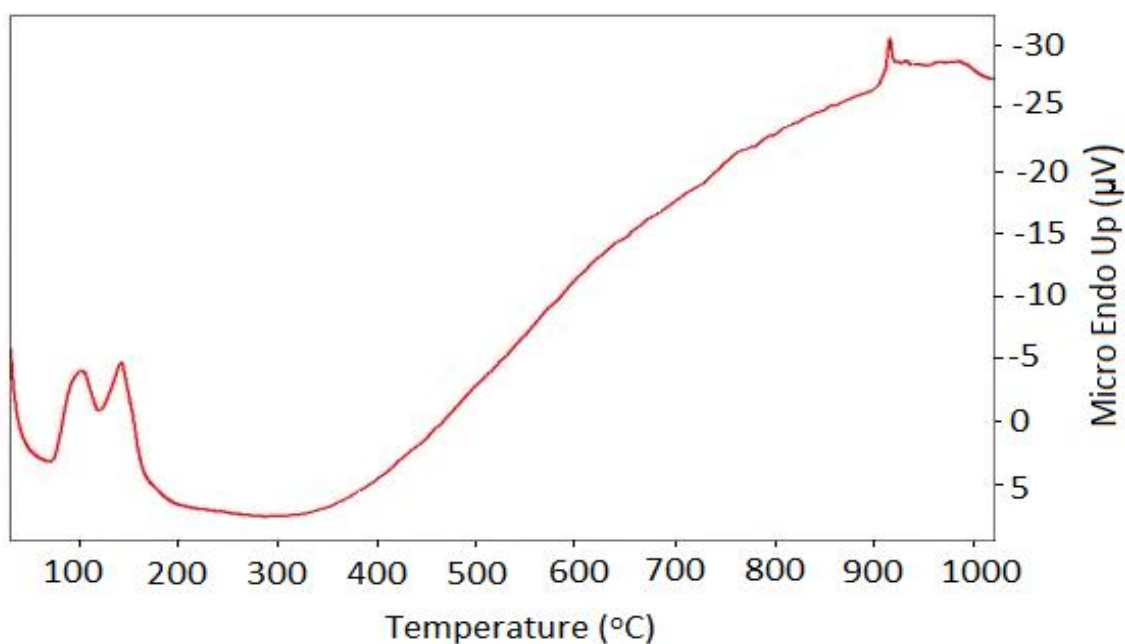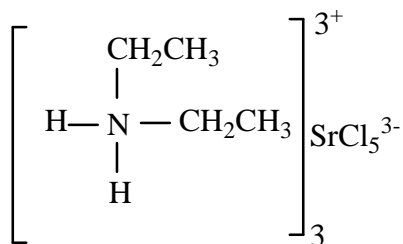

Figure 4. DTA thermogram of DEAPC-Sr crystal.

27

3.4 NMR spectroscopy analysis

(i) ^{1}H NMR spectrum

$$\left[\begin{array}{c} CH_2CH_3 \\ | \\ H-N-CH_2CH_3 \\ | \\ H \end{array}\right]_3^{3+} SrCl_5{}^{3-}$$

The ^{1}H NMR spectrum of DEAPC-Sr crystal is shown in Figure 5. The ^{1}H NMR spectrum exhibits three proton signals indicating the presence of three different proton environments.
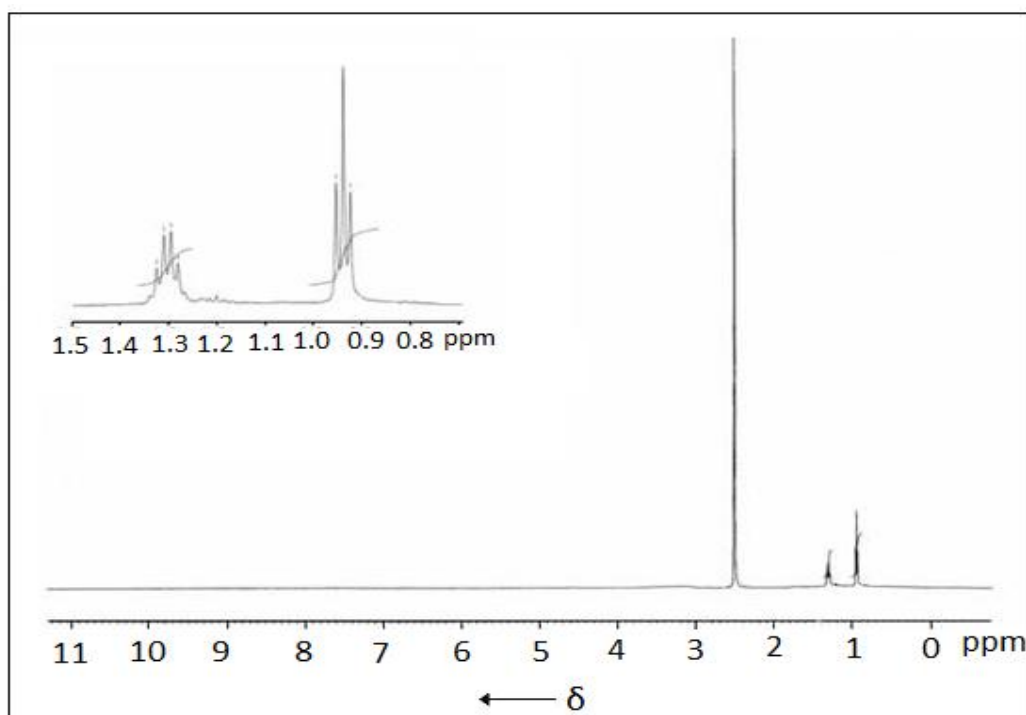

Figure 5. ^{1}H spectrum of DEAPC-Sr crystal.

The signal at 0.93 ppm is due to presence of methyl protons. The splitting of the signal into triplet is due to the coupling with two neighborhood protons of methylene group. The signal at 1.47 ppm is due to the presence of methylene protons. The splitting of the signal into quartet is due to lthe coupling with three neighborhood protons of methyl group. The signal at 2.5 ppm is the solvent peak.
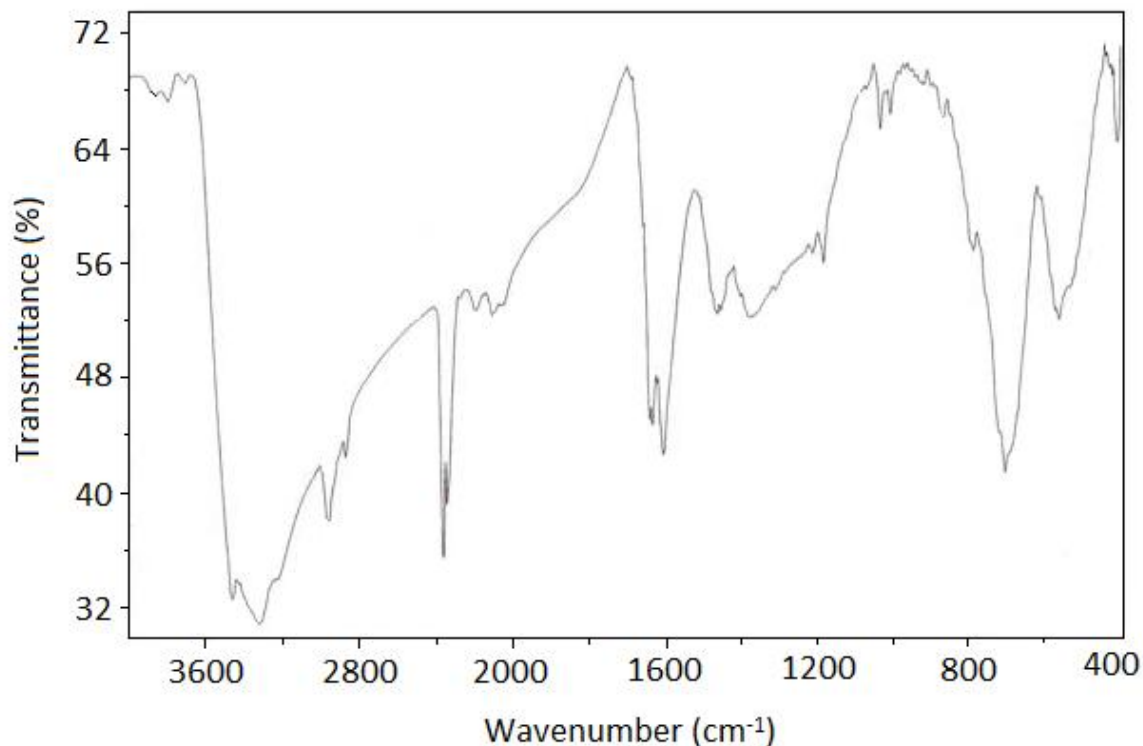
Table 3. FTIR spectral data of DEAPC-Sr crystal.

Frequencies (cm^{-1})	Assignments
3328	N-H asymmetric stretching vibration
2962	C-H stretching vibration
2360	Combination and overtone bands of primary ammonium salt
1631 and 1603	N-H bending vibration
1460	C-H deformation in CH_2 group.
1378	C-H deformation in CH_3 group
1033	C-N stretching vibration
702	N-H out-of-plane bending vibration
562	Skeletal vibration $SrCl_2^{2-}$

3.5 FTIR technique

The FTIR spectrum of grown DEAPC-Sr crystal is shown in Figure 6. The absorption frequencies and their assignments are given in Table 3. The absorption observed at 3328 cm^{-1} is due to the N-H asymmetric stretching vibration. The C-H stretching vibration is observed at 2962 cm^{-1}. The frequency at 2360 cm^{-1} is due to the combination and overtone bands of primary ammonium salt. The N-H bending vibration is observed at 1631 and 1603 cm^{-1}. The absorption at 1460 cm^{-1} is characteristics of C-H deformation in CH_2 group. The C-H deformation in CH_3 group is observed at 1378 cm^{-1}. The absorption at 1033 cm^{-1} is assigned to the C-N stretching vibration. The deformation out-of-plane vibration is observed at 702 cm^{-1} and the absorption at 562 cm^{-1} is due to skeletal vibration of $SrCl_2$. The vibrations of N-H asymmetric stretching, C-N stretching and skeletal vibration of $SrCl_2$ are important vibrations to confirm the formation of the crystal.

Figure 6. FTIR spectrum of DEAPC-Sr crystal.

29

3.6 Polarized Raman spectral study

The polarized Raman spectrum of grown DEAPC-Sr crystals is shown in Figure 7. The found at 3278 cm^{-1} is due to N-H stretching vibration. The C-H symmetric stretching vibration gives at 2905 cm^{-1}. The frequency at 1682 cm^{-1} is characteristics of N-H bending vibration. The C-H deformation in CH$_2$ group is observed peak at 1498 cm^{-1}. The frequency at 1385 cm^{-1} is due to C-H deformation in CH$_3$ group. The CH$_2$ twisting deformation mode of vibration is observed at 1291 cm^{-1}. The peak at 1110 cm^{-1} is assigned to C-N stretching vibration. The C-H out of plane bending vibration gives peak at 978 cm^{-1}. The frequency at 810 cm^{-1} is characteristics of C-H deformation mode. The small peak at 410 cm^{-1} may be due to C-C-C out of plane bending vibration. The C-C torsional bending vibration gives peak at 295 cm^{-1}. The peak at 48 cm^{-1} is assigned to lattice vibration of molecule.
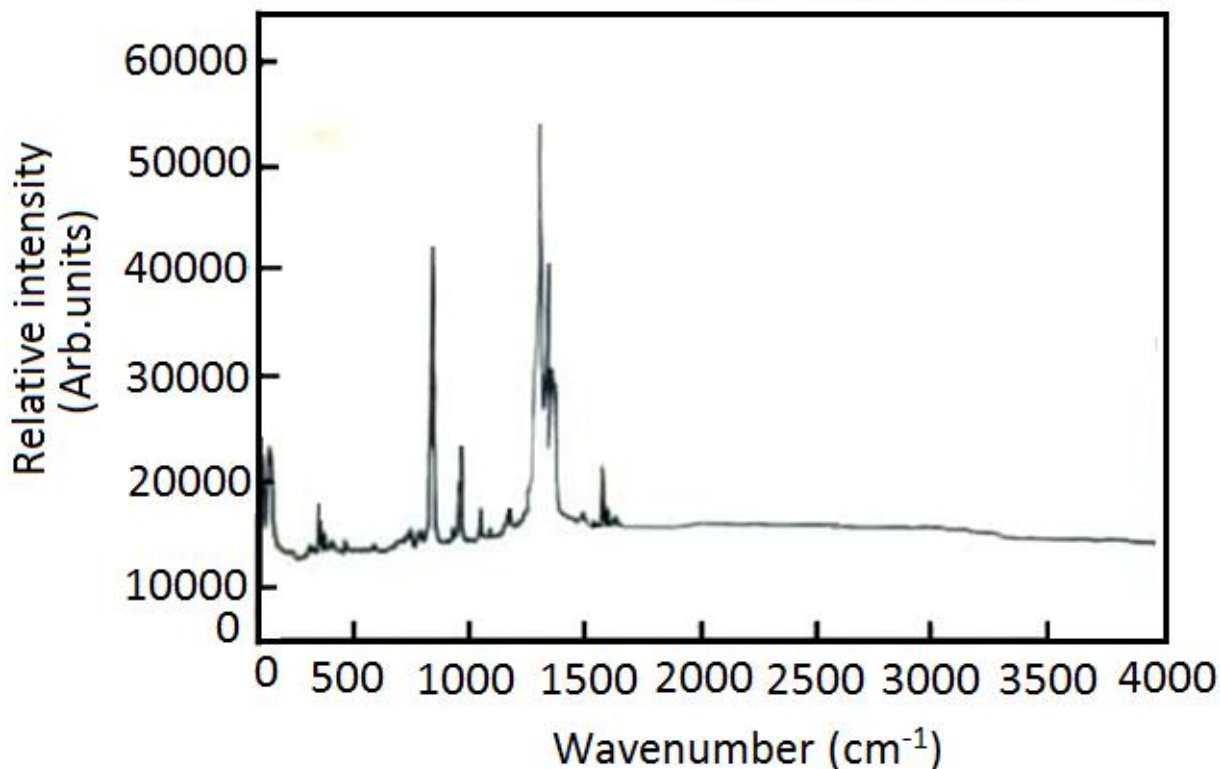

Figure 7. Polarized Raman spectrum of DEAPC-Sr crystal.

3.7 NLO study

The powder SHG efficiency of the crystal was studied using a mode locked Q-switched Nd:YAG laser by employing the modified Kurtz-Perry powder technique [10]. The fundamental beam of 1064 nm from Q-switched Nd:YAG laser pulse energy 6mJ/s with pulse width of 8 ns and repetition rate of 10 Hz was used to test the second harmonic generation. The output from Nd:YAG laser was used as illuminating source to the crystal specimen. The output from Q-switched laser was focused onto the crystals. Crystal DEAPC-Sr was powered with a uniform particle size and then packed in a microcapillay of uniform bore and exposed to laser radiation. Second harmonic radiation generated by the randomly oriented microcrystals was focused by a lens and detected by a photomultiplier tube. A sample of potassium dihydrogen phosphate (KDP) was used as a reference material. The emission of green light from the sample confirms the second NLO activity. Eventhough the material belongs to centrosymmetric class of crystals its NLO activity may be due to intense intermolecular hydrogen bonding and ordering of NH$_4^+$ ions within the crystal.

3.8 DFT study

Density Functional Theory (DFT) of chemical reactivity is known conceptual density functional theory. One of the aims of the conceptual density functional theory is to calculate the quantum chemical descriptors like hardness ( ), electronegativity ( ) and chemical potential (μ) giving useful hints about the stability of reactivity of chemical species. In this theory, aforementioned quantum chemical descriptors are calculated via following equations including ground state ionization energy and electron affinity values of chemical species (atoms, ions and molecules). Here it is important to note that electronegativity is described as the negative of chemical potential [11-14].

$$x = -\mu = 1 + A/2 \text{ ------}1$$
$$= 1 - A/2 \text{ ------------}2$$

Softness ( ) that is a measure of the polarisability of chemical species is defined as the multiplicative inverse of chemical hardness (=1/). Electrophilicity ( ) and nucleophilicity are two useful chemical reactivity indices. Parr who made many studies on chemical reactivity proposed the following formula to calculate the electrophilicity index depending on electronegativity and hardness values of chemical species. In addition, he described the nucleophilicity ( ) as the multiplicative inverse of electrophilicity (=1/)

$$= x^2/2 \text{ ------------}3$$

$$x = E_{HOMO} + E_{LUMO}/2 \text{ ------------}4$$
$$= E_{HOMO} - E_{LUMO}/2 \text{ ------------}5$$

The energies of the highest occupied molecular orbital (HOMO) and the lowest unoccupied molecular orbital (LUMO) are computed at various level. HOMO and LUMO orbitals for the crystal are shown Figure 8. The HOMO-LUMO energy gap reveals the intra-molecular charge transfer (ICT) interaction occurs within the molecule. The molecular electron repulsion orbital and molecular orbital of the crystal are given in Figure 9. The MEP surface picturizes the reactiveness against positive or negative reactants and attributes structure-activity relation of the system [15]. There exists a correlation between electrostatic potential and the dipole moment, electronegativity, and partial charges [16].
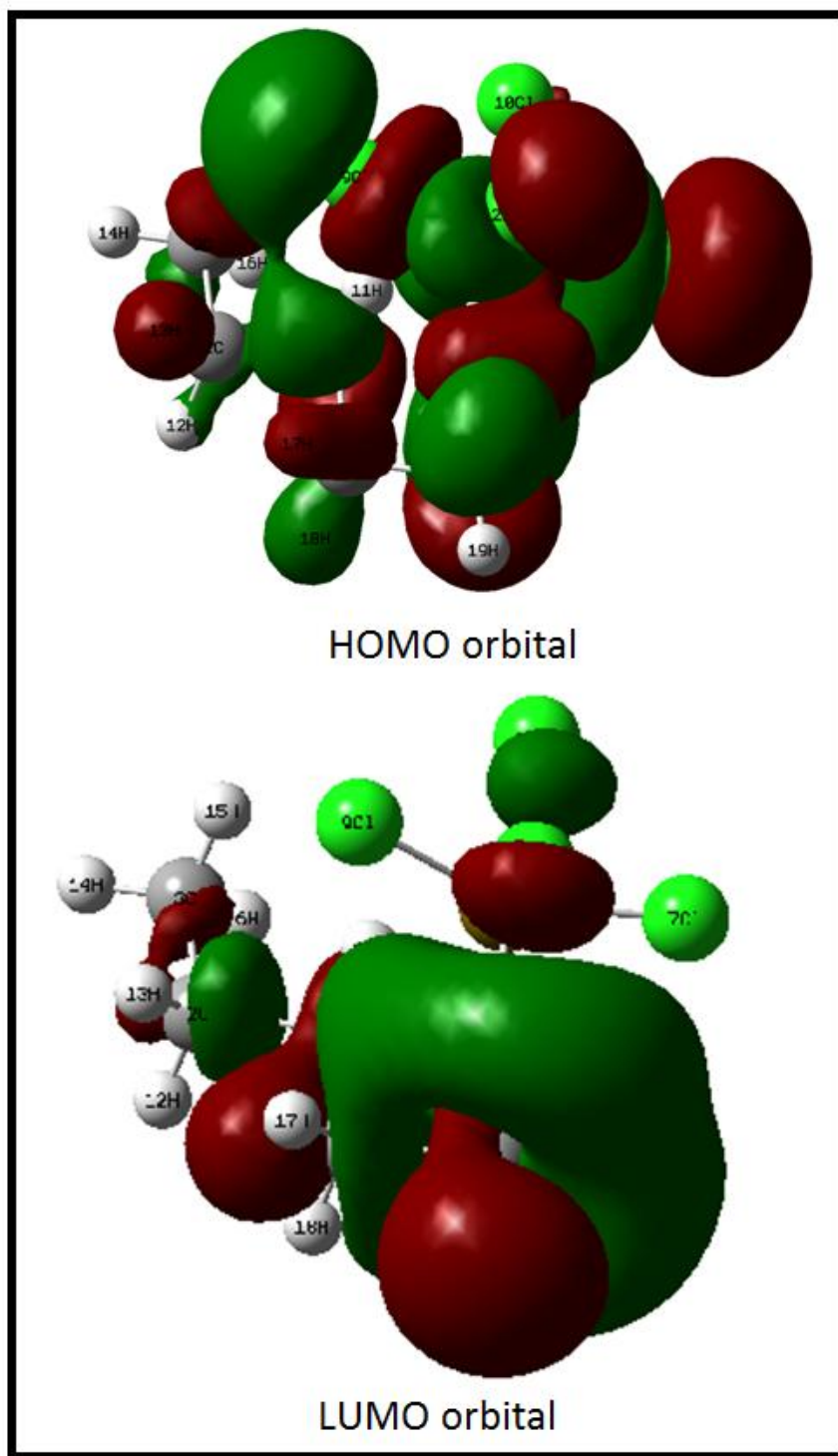
Figure 8. (a) HOMO orbital and (b) LUMO orbital of the crystal
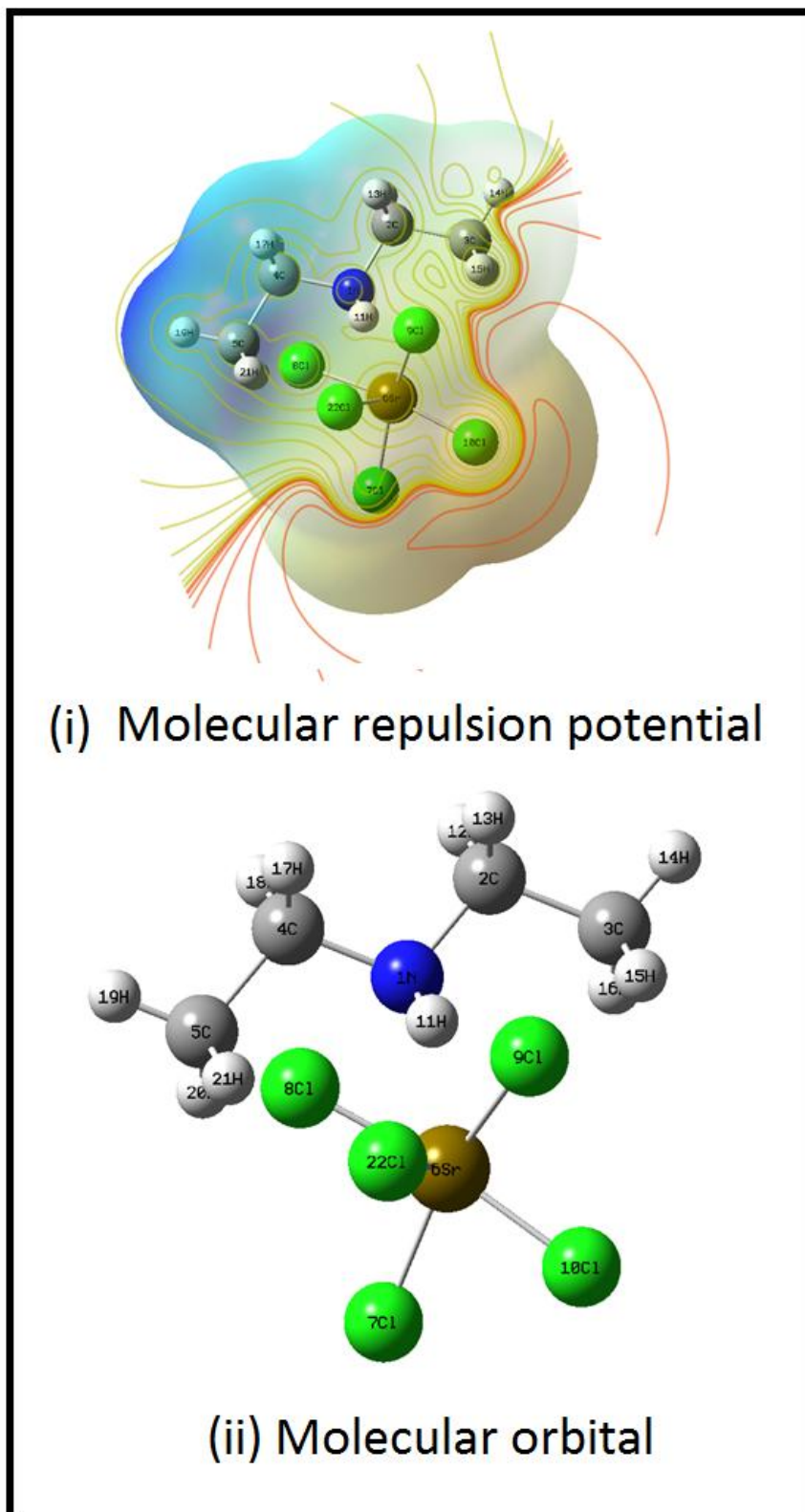
Figure 9. (a) Molecular electrostatic potential surfaces and (b) Molecular orbital of the crystal

4. Conclusions

Diethylammonium pentachlorostrontium(II) crystal was grown by slow evaporation solution growth method at ambient temperature. The grown crystals were bright, transparent and colourless. The elemental analysis and TG-DTG and DTA studies confirm the formation of the crystal in the stoichiometric ratio. The crystalline nature of the crystal was studied by Powder XRD method. The thermal studies also used to ascertain the decomposition pattern and thermal stability of the title crystal. The various chemical bonding and characteristic stretching vibrations of CN and $SrCl_2$ ions in the crystal mode of stretching vibrations of different molecular groups present in the crystal was identified by FTIR and polarized Raman spectral studies. The formation of the crystal and molecular structure was further confirmed by ^{1}H spectral study. The optical property of the crystal was determined by Kurtz-Perry powder technique. The DFT calculation study was studied to find out the HOMO-LUMO energy gap and intra-molecular charge transfer (ICT) interaction occurs within the molecule.

Acknowledgment

References

[1]   H. Z.Cummins, Phys. Rep. 185, 211 (1990).
[2]   G.Amirthaganesan, M.A.Kandhaswamy, M.Dhandapani, Cryst. Res. Technol. 42, No. 7, 684 (2007).
[3]   A.Sawada, J.Sugiyama, M.Wada, Y.Ishibashi, J.Phys.Soc.Jpn. 48, 1773 (1980).
[4]   K.Gesi, J.Phys.Soc.Jpn. 51, 203 (1982).
[5]   K.Gesi, Ferroelectrics, 285, 139 (2003).
[6]   M.L.Bansal, V.C.Sahni, A.P.Roy, J.Phys.Chem.Solids, 40, 109 (1979).
[7]   A.P.Roy, V.C.Sahni, M.L.Bansal, J.Phys.Chem.Solids, 40, 289 (1979).
[8]   K.Byrappa, M.A.Kandhaswamy, V.Srinivasan, Cryst.Res.Technol. 34, 843 (1999).
[9]   J.L.Burries, L.Tereschenko, P. Kabos, H.D. Hochheimer, Y. Lupsin, C.R. Evenson, J.Phys Chem.Solids, 61, 719 (2000).
[10]   S.K.Kurtz, T.T.Perry A Powder Technique for the Evaluation of Nonlinear Optical Materials. J.App.Phy. 39, 3798 (1968).
[11]   R.G.Pearson, J. Am. Chem. Soc. 85, 3533 (1963).
[12]   R.G.Pearson, Inorg. Chem. 27, 734 (1988).
[13]   R.G.Parr, L.V.Szentpaly, S.Liu, J.Am.Chem. Soc. 121, 1922 (1999).
[14]   T.Koopmans, Physica, 1, 104 (1934).
[15]   A.M.Fatmah Al-Omary, Y.Sheena Mary, C.Yohannan Panicker Ali, A.El-Emam Ibrahim, A.Al-Swaidan Abdulaziz, A. Al-Saadi and C.Van Alsenoy, J.Mol.Struct. 1096, 1 (2015).

[16] J.Devi, M.Yadav, D.Kumar, L.S.Naik, D.K. Jindal, Appl.Organo.Chem. 33, 1 (2018).

Access this Article in Online	
	Website: www.ijcrcps.com
	Subject: Chemistry
Quick Response Code	
DOI: 10.22192/ijcrcps.2023.10.06.002	